Hadron Nuclear Physics (HNP2013)
International Journal of Modern Physics: Conference Series
Vol. 29 (2014) 1460221 (9 pages)

DOI: 10.1142/S201019451460221X

Nuclear equation of state with the variational method and its application to supernova simulations

Hajime Togashi

Department of Pure and Applied Physics, Waseda University
3-4-1 Okubo Shinjuku-ku, Tokyo 169-8555, Japan
hajime_togashi@ruri.waseda.jp

Masatoshi Takano

Research Institute for Science and Engineering, Waseda University
3-4-1 Okubo Shinjuku-ku, Tokyo 169-8555, Japan

Department of Pure and Applied Physics, Waseda University,
3-4-1 Okubo Shinjuku-ku, Tokyo 169-8555, Japan
takanom@waseda.jp

Kohsuke Sumiyoshi

Numazu College of Technology
Ooka 3600, Numazu, Shizuoka 410-8501, Japan
sumi@numazu-ct.ac.jp

Ken'ichiro Nakazato

Department of Physics, Faculty of Science and Technology,
Tokyo University of Science, Yamazaki 2641, Noda, Chiba 278-8510, Japan
nakazato@rs.tus.ac.jp

Published 16 April 2014

We report on an equation of state (EOS) of hot asymmetric nuclear matter constructed using the variational method and its application to hydrodynamic simulations of core-collapse supernovae. This nuclear EOS is based on the AV18 two-body potential and UIX three-body potential, and the energy per nucleon at zero temperature is constructed with the cluster variational method. At finite temperatures, the free energies per nucleon are calculated with an extension of the variational method devised by Schmidt and Pandharipande. This EOS is in good agreement with that by the Fermi hypernetted chain variational calculations at zero and finite temperatures, and the structure of neutron stars calculated with this EOS is consistent with recent observational data. Using this nuclear EOS, we perform a spherically symmetric general-relativistic adiabatic simulation of the SN explosion. The explosion energy calculated with our EOS in the present simulation is larger than that obtained with the Shen EOS, implying that the variational EOS is softer than the Shen EOS.

Keywords: Nuclear matter; nuclear EOS; variational method; neutron stars; supernovae.

PACS Numbers: 21.65.−f, 21.65.Cd, 21.65.Mn, 26.50.+x, 26.60.−c

1. Introduction

The equation of state (EOS) for dense nuclear matter is one of the important topics in the study of high-energy astrophysical objects. For example, the structure of neutron stars (NSs) is governed by the nuclear EOS at zero temperature. In fact, a number of EOSs of cold nuclear matter, calculated either with many-body theories starting from the realistic nuclear Hamiltonian or with phenomenological nuclear models, have been applied to NSs, and compared with observational data. The nuclear EOS is also important to the study of core-collapse supernovae (SNe). In contrast to the case of NS studies, however, the nuclear EOSs that are available for SN simulations are limited, because an SN-EOS must cover a wide range of densities, proton fractions and temperatures. Typical hot nuclear EOSs which are available for numerical simulations of SNe are the Lattimer-Swesty EOS[1] and the Shen EOS.[2] The former is based on a Skyrme-type interaction for uniform nuclear matter and a compressible liquid drop model for non-uniform matter. The latter is based on the relativistic mean field theory for uniform matter and the Thomas-Fermi approximation for non-uniform matter. In recent years, the number of nuclear EOSs available for SN simulations has increased, but these SN-EOSs are based on phenomenological models for uniform matter. Nuclear EOSs constructed with many-body calculations starting from the realistic nuclear Hamiltonian have not yet been applied to SN simulations, as they have been in NS studies.

Under these circumstances, we are now constructing a new nuclear EOS applicable to SN simulations using the variational many-body theory starting with realistic nuclear forces. A typical variational method is the Fermi hypernetted chain (FHNC) method, which has been applied to symmetric nuclear matter and pure neutron matter. However, it is difficult to calculate the EOS of asymmetric nuclear matter for arbitrary proton fractions with the FHNC method. On the other hand, in SN simulations, an EOS for hot asymmetric nuclear matter is necessary. Therefore, in our project, we employ a simplified cluster variational method to construct an EOS for uniform asymmetric nuclear matter.

In this paper, we report on the nuclear EOS which we have recently constructed with our variational method, and on an application of this variational EOS to a test numerical simulation of a core-collapse SN.

2. The Variational EOS of Hot Asymmetric Nuclear Matter

In this section, we describe the variational calculations for uniform asymmetric nuclear matter at zero and finite temperatures. As stated above, we employ a simplified cluster variational method in order to construct an EOS table for various densities, temperatures and proton fractions.

We start from the realistic nuclear Hamiltonian, which is the sum of the two-body Hamiltonian H_2 and the three-body Hamiltonian H_3. Since the FHNC method for infinite fermion systems, in which two fermions interact through two-body strong short-range forces, have been developed and established over many years, results achieved with this variational method are fairly reliable. Therefore, we first calculate the expectation value of H_2 per nucleon using the cluster variational method, and confirm that the obtained energies per nucleon reproduce the results found with the FHNC method.

The two-body Hamiltonian H_2 is expressed as

$$H_2 = -\sum_{i=1}^{N} \frac{\hbar^2}{2m} \nabla_i^2 + \sum_{i<j}^{N} V_{ij}, \tag{1}$$

where m is the mass of the nucleon, and the two-body nuclear potential V_{ij} is chosen as the isoscalar part of the AV18 potential. The expectation value of H_2 is calculated with the Jastrow wave function

$$\Psi = \mathrm{Sym}\left[\prod_{i<j} f_{ij}\right] \Phi_{\mathrm{F}}. \tag{2}$$

Here f_{ij} is the two-body correlation function composed of the spin-isospin-dependent central, tensor and spin-orbit correlation functions, which may depend also on the third component of the two-nucleon total isospin so as to take into account the medium effects. In Eq. (2), Φ_{F} is the degenerate Fermi gas wave function at zero temperature, which is specified by the occupation probabilities of single-nucleon states $n_{0i}(k) = \theta(k_{\mathrm{F}i} - k)$ $(i = \mathrm{p, n})$, with k_{Fp} and k_{Fn} being the Fermi wave numbers of protons and neutrons, respectively. Using this Jastrow wave function Ψ for a given set of the nucleon number density ρ and proton fraction Y_{p}, we evaluate the two-body energy per nucleon E_2/N as the expectation value of H_2 in the two-body cluster approximation, i.e., we take into account only two-body cluster terms, and neglect the higher-order cluster terms. Then, we minimize E_2/N with respect to the spin-isospin-dependent correlation functions by solving the Euler-Lagrange equations. In this minimization, we impose the extended Mayer's condition and the healing distance condition so that E_2/N for symmetric nuclear matter ($Y_{\mathrm{p}} = 0.5$) and pure neutron matter ($Y_{\mathrm{p}} = 0$) reproduce the corresponding expectation values of H_2 from the FHNC calculations by Akmal et al.[3] (APR).

Next, we calculate the contribution from the three-body Hamiltonian H_3 as follows. We first express the three-body energy per nucleon E_3/N based on the expectation value of H_3 constructed with the UIX three-body potential using the Fermi-gas wave function. Then, with use of the uncertainty in the three-body forces, we introduce four parameters in E_3/N, so as to take into account the corrections that are included in the FHNC calculations, somewhat phenomenologically. The

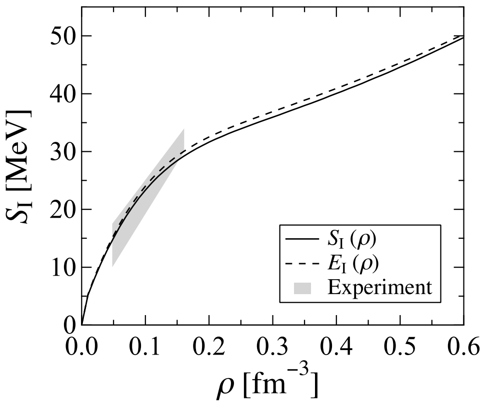

Fig. 1. The density-dependent symmetry energy S_I as a function of the nucleon number density ρ. E_I is also shown. The shaded region shows the experimental data obtained from heavy ion collisions.

values of these parameters are determined such that the total energy per nucleon $E/N = E_2/N + E_3/N$ reproduces the empirical saturation data, i.e., the saturation density $\rho_0 = 0.16$ fm^{-3}, saturation energy $E_0 = -16.09$ MeV, incompressibility $K = 245$ MeV and symmetry energy $E_\mathrm{sym} = 30.0$ MeV. The E/N obtained for symmetric nuclear matter and pure neutron matter are in good agreement with the results of APR.[4] Validity of the treatment of E_3/N is examined in Ref. 5.

The density-dependent symmetry energy S_I, which is derived from E/N as

$$S_\mathrm{I} \equiv \frac{1}{8}\frac{\partial^2}{\partial Y_\mathrm{p}^2}\frac{E}{N}\bigg|_{Y_\mathrm{p}=1/2}, \tag{3}$$

is shown in Fig. 1 as a function of ρ. Also shown is the energy difference E_I between E/N of pure neutron matter ($Y_\mathrm{p} = 0$) and that of symmetric nuclear matter ($Y_\mathrm{p} = 0.5$), i.e.,

$$E_\mathrm{I} \equiv \frac{E(\rho, Y_\mathrm{p} = 0)}{N} - \frac{E(\rho, Y_\mathrm{p} = 1/2)}{N}. \tag{4}$$

It is obvious that S_I and E_I are identical if E/N at a fixed ρ increases quadratically with Y_p from symmetric nuclear matter to pure neutron matter. Validity of the approximation $S_\mathrm{I} = E_\mathrm{I}$, which has been adopted by many researchers, is confirmed in the present study, as shown in Fig. 1, though a slight difference between the two quantities can also be seen. In Fig. 1, the shaded region shows the experimental data on the symmetry energy obtained from the heavy ion collisions;[6] the symmetry energy of this variational EOS is consistent with those experimental data.

Next, we discuss the NSs using the present EOS. For non-uniform matter, we adopted the crust EOS constructed in the Thomas-Fermi approximation reported in Ref. 7. The maximum mass of the NSs calculated with this EOS is 2.22 $M_\odot$, which is consistent with the observational data on the masses of heavy NSs.[8] Furthermore, the NS radii are also consistent with the observationally suggested values from the analysis by Steiner *et al.*[9] as shown in Ref. 10.

For hot nuclear matter, we calculate the free energy per nucleon F/N at temperature T with an extension of the variational method proposed by Schmidt and Pandharipande (SP).[11] In this method, F/N is expressed as

$$\frac{F}{N} = \frac{E_{0\mathrm{T}}}{N} - T\frac{S_0}{N}, \tag{5}$$

where $E_{0\mathrm{T}}/N$ is the approximate internal energy per nucleon and S_0/N is the approximate entropy per nucleon. $E_{0\mathrm{T}}/N$ is composed of the two-body energy part $E_{2\mathrm{T}}/N$ and the three-body energy part $E_{3\mathrm{T}}/N$. Following the method of SP, $E_{2\mathrm{T}}/N$ is obtained by replacing the occupation probabilities of the single particle states $n_{0i}(k)$ in the two-body energy at zero temperature E_2/N by the average occupation probabilities $n_i(k)$ expressed as

$$n_i(k) = \left\{1 + \exp\left[\frac{\varepsilon_i(k) - \mu_{0i}}{k_{\mathrm{B}}T}\right]\right\}^{-1}. \tag{6}$$

Here, quasi-nucleon energies $\varepsilon_i(k)$ are specified by their effective masses m_i^* as $\varepsilon_i(k) = \hbar^2 k^2/2m_i^*$. For simplicity, the three-body energy $E_{3\mathrm{T}}/N$ is assumed to be the same as E_3/N at zero temperature. The approximate entropy S_0/N in Eq. (5) is also expressed by $n_i(k)$ as in the case of a non-interacting quasi-nucleon gas. Then, F/N is minimized with respect to m_{p}^* and m_{n}^*.

The calculated F/N for symmetric nuclear matter and pure neutron matter are in good agreement with those obtained from the FHNC calculations by Mukherjee;[12] furthermore, other thermodynamic quantities, such as the entropy, internal energy, pressure and chemical potentials, which are obtained from F/N through thermodynamic relations, are reasonable, as reported in Ref. 10. Those thermodynamic quantities are necessary to construct an SN-EOS.

3. Application of the Variational EOS to Core-Collapse SNe

In this section, we apply the present EOS to a hydrodynamical simulation of core-collapse SNe. We employ the numerical code for the spherically symmetric general-relativistic hydrodynamical simulation given in Ref. 13, and neglect weak reactions in the simulation, i.e., we fix the electron fraction of each fluid element at the initial value. Since the energy loss due to the neutrino emission is not taken into account, this simulation is fully adiabatic. Next, we construct an SN-EOS based on the variational EOS described in the last section. Since an SN-EOS must treat not only uniform but also non-uniform matter, we adopt the Shen EOS for non-uniform matter at low densities, and connect it to the variational EOS of high-density uniform matter. Starting from the 15 $M_\odot$ progenitor model of Ref. 14, we perform the SN simulation. In this simulation, the SN explosion is successful, as seen below.

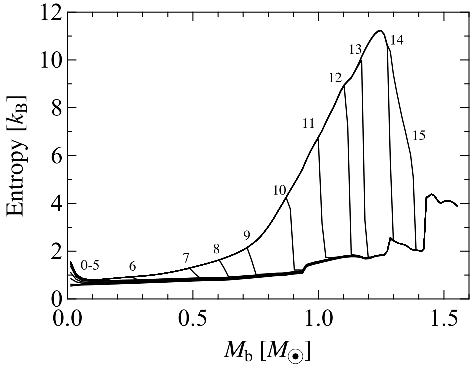

Fig. 2. The entropy profiles at selected times as functions of the baryon mass coordinate M_b. The numbers denote the time sequence as explained in the text.

Figure 2 shows the evolution of the entropy profile; the entropy per baryon is given as a function of the baryon mass coordinate M_b in units of $M_\odot$. Here, M_b represents the time-dependent radius of the enclosed baryon mass; for a more precise definition, see the Appendix of Ref. 15. The numbers in Fig. 2 denote the time sequence, and the number (10) corresponds to the time of the bounce. The explicit times that correspond to each number are shown in Table 1, where we define the time t_{pb} to be zero at the bounce. From this figure, it is seen that as the shock wave propagates toward the surface of the core, the entropy behind the shock increases steeply. In the early stages, the entropy in the central region remains at $\sim 1k_B$ because of the adiabatic collapse. At the bounce, the entropy reaches about 4 k_B just behind the shock at $M_b \sim 0.9M_\odot$; then, at $t_{pb} = 5$ ms (corresponding to the number (14)), the shock reaches at $M_b \sim 1.3M_\odot$ with the entropy being higher than 10 k_B. It should be pointed out that the shock reaches the surface of the core, which implies the success of the stellar explosion in this model case.

Figure 3 shows the evolution of the temperature profile: The numbers denote the time sequence as in Fig. 2. In this figure, it can be seen that the temperature increases to about 5 MeV in the early stages of the collapse (the numbers 0-5), and as the pressure wave propagates toward the outside, the temperature behind the pressure wave increases steeply. At the bounce, the temperature becomes more than 20 MeV at $M_b \sim 0.9M_\odot$. The peak of the temperature moves toward the surface of the core, and the temperature of the inner region remains at $\sim$ 10 MeV.

Table 1. Times corresponding to the numbers in Figs. 2 and 3.

Number	0	1	2	3	4	5	6	7
Time t_{pb} [ms]	−1.00	−41.4	−6.18	−1.84	−0.58	−0.40	−0.30	−0.20
Number	8	9	10	11	12	13	14	15
Time t_{pb} [ms]	−0.15	−0.10	0.00	0.15	0.50	1.00	5.00	25.0

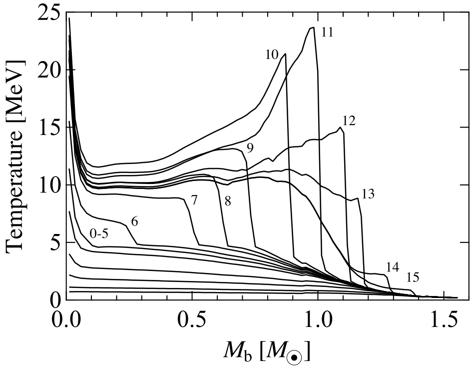

Fig. 3. The temperature profiles at selected times as functions of the baryon mass coordinate M_b. The numbers denote the time sequence as explained in the text.

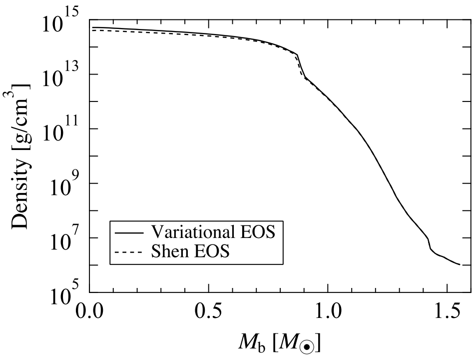

Fig. 4. The density profile at $t_\mathrm{pb} = 0$ ms as a function of the baryon mass coordinate M_b. The result obtained with the Shen EOS is also shown.

Figure 4 shows the density profile in the core at the time of the bounce with the present EOS; for comparison, in this figure we also show the density profile at the bounce calculated using the Shen EOS. The central density at the bounce with the variational EOS reaches 5.2×10^{14} g/cm^3, which is larger than that calculated with the Shen EOS (4.0×10^{14} g/cm^3); this result indicates that the present EOS is softer than the Shen EOS.

Figure 5 shows the profile of the radius at the bounce with both the variational and Shen EOSs. It can be seen that the radius calculated with the variational EOS is slightly smaller than that obtained with the Shen EOS for the inner region $M_\mathrm{b} \lesssim 0.9 M_\odot$; the high-density core region is smaller with the present variational EOS, again because this EOS is softer. These results imply that the high-density central core described with the variational EOS is more compact than that described with the Shen EOS. Correspondingly, the released explosion energy calculated with

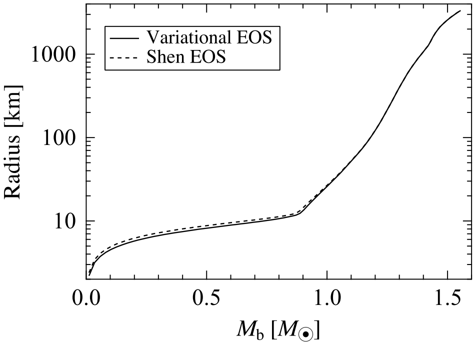

Fig. 5. The profile of the radius at $t_{\rm pb} = 0$ ms as a function of the baryon mass coordinate $M_{\rm b}$. The result obtained with the Shen EOS is also shown.

the variational EOS (1.7×10^{51} erg) is larger than that of the Shen EOS (1.5×10^{51} erg).

4. Summary and Concluding Remarks

In this paper, we presented an EOS of uniform asymmetric nuclear matter at zero and finite temperatures which we constructed with the cluster variational method, and then applied it to a spherically symmetric numerical simulation of adiabatic core-collapse SNe. Our EOS is based on the realistic nuclear Hamiltonian composed of the AV18 and UIX potentials. The obtained energy per nucleon E/N is in good agreement with that obtained by Akmal et al.(APR), and the symmetry energy is consistent with the experimental data on heavy ion collisions. Furthermore, the masses and radii of NSs calculated with the present EOS are consistent with observational data. Free energies per nucleon F/N calculated with an extension of the variational method proposed by Schmidt and Pandharipande are in good agreement with those obtained by the FHNC calculations, and other thermodynamic quantities derived from F/N obtained via thermodynamic relations are reasonable.

Next, we applied the variational EOS to a relatively simple hydrodynamical simulation of core-collapse SNe. We performed a spherically symmetric general-relativistic adiabatic simulation without neutrino transfer, as a test for application to SN simulations. We found that the numerical code runs successfully with the variational EOS, and succeeded in achieving a prompt explosion with this adiabatic calculation. The central mass density at the bounce with the variational EOS is higher than that found with the Shen EOS, and the radius of the inner core calculated with the variational EOS is smaller, i.e., the variational EOS is softer than the Shen EOS in these adiabatic simulations. The next step is to perform a spherically symmetric general-relativistic simulation in which neutrino transfer is taken into account; we plan to complete this simulation and report the results in a future paper.

It should be noted that, in the present simulation, the Shen EOS is used for non-uniform matter, which is inconsistent with the uniform variational EOS. Therefore, to further this work, one of our most important tasks is to construct the EOS of non-uniform matter in a self-consistent manner. We are now proceeding with the construction of an EOS for non-uniform matter in the Thomas-Fermi approximation using the present EOS, by following the procedure adopted in the Shen EOS.

Acknowledgments

The numerical computations in this work were carried out on SR16000 at YITP in Kyoto University and on the GPGPU and SR16000 at the High Energy Accelerator Research Organization (KEK). This work is supported by JSTS (Nos. 21540280, 22540296, 24244036, 25400275), JSPS Research Fellowships for Young Scientists (No. 24-3275), and the Grant-in-Aid for Scientific Research on Innovative Areas of MEXT (Nos. 20105003, 20105004, 20105005, 24105008).

References

1. J. M. Lattimer and F. D. Swesty, *Nucl. Phys. A* **535**, 331 (1991).
2. H. Shen, H. Toki, K. Oyamatsu and K. Sumiyoshi, *Nucl. Phys. A* **637**, 435 (1998).
   H. Shen, H. Toki, K. Oyamatsu and K. Sumiyoshi, *Prog. Theor. Phys.* **100**, 1013 (1998).
   H. Shen, H. Toki, K. Oyamatsu and K. Sumiyoshi, *Astrophys. J. Suppl.* **197**, 20 (2011).
3. A. Akmal, V. R. Pandharipande and D. G. Ravenhall, *Phys. Rev. C* **58**, 1804 (1998).
4. H. Kanzawa, K. Oyamatsu, K. Sumiyoshi and M. Takano, *Nucl. Phys. A* **791**, 232 (2007).
5. M. Takano, H. Togashi, S. Yamamuro, K. Nakazato and H. Suzuki, *AIP Conf. Proc.* **1484** (2012) 378.
6. M. B. Tsang et al., *Prog. Part. Nucl. Phys.* **66**, 400 (2011).
   M. B. Tsang et al., *Phys. Rev. Lett.* **102**, 122701 (2009).
7. H. Kanzawa, M. Takano, K. Oyamatsu and K. Sumiyoshi, *Prog. Theor. Phys.* **122**, 673 (2009).
8. P. B. Demorest, T. Pennucci, S. M. Ransom, M. S. E. Roberts and J. W. T. Hessels, *Nature* **467**, 1081 (2010).
   J. Antoniadis et al., *Science* **340**, 1233232 (2013).
9. A. W. Steiner, J. M. Lattimer and E. F. Brown, *Astrophys. J.* **722**, 33 (2010).
10. H. Togashi and M. Takano, *Nucl. Phys. A* **902**, 53 (2013).
11. K. E. Schmidt and V. R. Pandharipande, *Phys. Lett. B* **87**, 11 (1979).
    A. Mukherjee and V. R. Pandharipande, *Phys. Rev. C* **75**, 035802 (2007).
12. A. Mukherjee, *Phys. Rev. C* **79**, 045811 (2009).
13. S. Yamada, *Astrophys. J.* **475**, 720 (1997).
14. S. E. Woosley and T. Weaver, *Astrophys. J. Suppl.* **101**, 181 (1995).
15. K. Sumiyoshi, H. Suzuki, S. Yamada and H. Toki, *Nucl. Phys. A* **730**, 227 (2004).